Study of positive parity states form factors for ^{17}O nucleus with Skyrme-Hartree-Fock method.

Awara Rasul Mohammed, Aziz H. Fatah[*]

Department of physics, College of Science, University of Sulaimanya, Sulaimanya, Iraq.
Corresponding author : ✉ : aziz.fatah@univsul.edu.iq.

CrossMark

Abstract

Elastic and inelastic electron scattering form factors for the ^{17}O nucleus are calculated for the positive parity low-lying states in the momentum transfer interval 0.05-3 fm^{-1} in the framework of shell model and Skyrme-Hartree-Fock calculations. Also, protons, neutrons, mass and charges root mean square, r.m.s., radii and the charge spatial density distribution are calculated. The ZBME model space out of ^{12}C nuclei core with rewile interaction have been used. For all selected ground and excited states, Skyrme interactions with SkXcsb and SLy4 parameter, harmonic and Wood-Saxon potentials are adopted in Hartree-Fock theory to generate the mean potential and hence calculate the elements of single-particle matrix and form factors. Also, we have used Tassie model to account for core-polarization effect. Finally, to check the reality of the calculated values, the charges r.m.s. and form factors are discussed and compared to the measured values. A good agreement can be shown by the theoretical results to the measured ones.

1. Introduction:

Electron scattering (ES) is considered by a strong tool for investigation of the nuclei properties and structures, and it offers a major source of experimental data to check the reality of theoretical calculations and models for nuclear ground and excited states [1], [2]. Additionally, it offers the most accurate data on nuclear size, charge distribution, and electromagnetic current distributions inside the nucleus [3].

The first-born approximation in which one photon exchanges with the nucleus, is considered to be a successful approximation for tiny α ($Z\alpha \ll 1$), is the framework in which we perform our computations [4], where Z denotes the atomic number. Also we divided the ^{17}O nucleus shells into the ^{12}C core and the model space (valence) shells, the core nucleons have been put to be non-interacting and only

taken the interactions of valence nucleons, we take care this problem by introducing nucleons effective charges. Applying the effective charges plays the role of polarizing the protons of core by the valence neutrons and protons and mostly called the core-polarization effect (CPE) [4].

Because the nuclear system is complex, for the simplicity of calculation we divide in to three parts, the core part which is make from some or all closed shells, the model space which consists of some states out of the closed core, and the extra space which are the remnant states beyond the model space. We put the core nucleons to be inert, that is non-interacting, while indeed they have grate contribution in interaction. So we have to correct this approximation. We do this through a model called Coulomb valance Tassie model (CVTM) or simply Tassie model (TM) through NushellX@MSU code which treats this through nucleon effective charges that enables uniform mass distribution and charge density. This process called core-polarization effect in which the core nucleons due to interaction with the incident electron jump to excited states and the core will be polarized [5].

The first experiment in electron excitation of nuclei was

done by Collins and Waldman in 1940, while the first theoretical treatment was pointed out by Mamasachlisov in 1943 [6]. The nucleus ^{17}O have about 112 excited states under 24 MeV excitation level [7]. This isotope of oxygen thus offers a great possibility to understand the abundant level structure of the light and stable nucleus [8], [9]. Many theoretical and experimental research have been done to explore the static and dynamic properties of this fascinating system of nucleons. In 1975, the first work was done by Kim et al. [9] to study the inelastic ES for ^{17}O at momentum transfers 0.6 up to 1.1 fm^{-1}.

The transverse form factor (FF) for the ^{17}O nucleus ground state has been determined through elastic ES in the effective momentum transfer interval 0.55-2.8 fm^{-1} by Hynes et al. [10]. Hicks [11] theoretically found the root mean square (r.m.s.) radii with M1 and M3 multipoles FFs for the $1d_{5/2}$ ^{17}O neutron state. He also drew the information on the distinction the M3 and M5 contributions quantitatively.

The radial algebraic wave function parameters which are correspondent to the ^{17}O nucleus valence neutron state of $1d_{5/2}$ have been calculated by Coon and Jaqua [12] via fitting to the magnetic ES data at high momentum transfer. Radhi et al. [13] investigated the transverse FFs of elastic magnetic ES for the odd-A stable nuclei including ^{17}O at $5/2^+$ state in the sd configuration, taking into consideration CPEs. Elastic scattering for ^{17}O has been studied by Han et al. [14]. E. Strano et al. [15] observed the ground state scattering for ^{17}O on 58Ni nuclei at some different energies. Alzubadi et al. [7] studied the transition probabilities, energy levels and FFs for both elastic and inelastic ES for states close to ground state of positive and negative parities in the momentum transfer 0.5 upto 1.5 fm^{-1}. Inelastic ES for nucleus 17O has been studied by taking in to account the higher states outside ^{16}O core by Abbas et al. [16]. El-Hammamy et al. [17] analyzed the ^{17}O $+^{17}$Pb ES at energies of 78 and 90.4 MeV.

The aim of the current work is to calculate protons, neutrons, mass and charges r.m.s. radii, the charge spatial density distribution, and ESFFs for positive low-lying parity states for the momentum transfer values from 0.05 to 3 fm^{-1} with 0.05 fm^{-1} resolution. The ZBME model space has been used for the core ^{12}C and the interaction type used is rewile Hamiltonian which is used for generate the positive parity states actual wave functions. As a correction for core nucleons which have been put as inert, non-interacting, we use CPE through Tassie model.

1.1 Theory and methodology:

The ESFF decomposed in to longitudinal component, F_L (q), and a transverse one, F_T (q). They depend only on momentum transfer q and energy loss ω, but not on scattering angle θ. They can be divided into different multipoles contributions [18]:

$$|F_L(q)|^2 = \sum_{J \geq 0} |F_J^C(q)|^2$$
$$|F_T(q)|^2 = \sum_{J \geq 1} |F_J^E(q)|^2 + |F_J^M(q)|^2 \tag{1}$$

where F_J^C, F_J^E, and F_J^M are longitudinal, transverse electric, and magnetic transition FFs with multipolarity J respectively. The permitted values for J in eq.(1) are limited by $|J_i - J_f| \leq J \leq J_i + J_f$, where $J_i = 5/2$ is the ground state total angular momentum and J_f is those for excited states of ^{17}O nucleus. Two other electromagnetic selection rules restrict the values of J further, which are the parity conservation rules. They are $(-1)^J$ for electric (CJ,EJ) interactions and $(-1)^{J+1}$ for magnetic (MJ) interactions [8]. The longitudinal and transverse FFs could be represented with respect to double bar matrix elements of the electromagnetic transition operators of ES [8].

$$|F_j^\eta(q)|^2 = \frac{4\pi}{Z^2(2J_i + 1)} \sum_{t_Z} e(t_Z) \left| \langle J_f || \hat{T}_{J:t_Z}^\eta(q) || J_i \rangle \right|^2 F_{cm}^2(q)$$
$$F_{fs}^2(q) \tag{2}$$

Here η = C, E, M, β = 1 for η = C and $\beta = \sqrt{(J+1)/J}$ for η = E, M. And J_i and J_f are respective initial and final nuclear states. $\hat{T}_{J:t_z}^\eta(q)$ denotes each of Coulomb, transverse electric and magnetic multiple operators of ES respectively. $F_{cm}^2(q)$ represents the translational-invariance lack, center of mass, correction in the shell model and $F_{fs}(q)$ is the FF for finite size of nucleons (fs). The double bar ES operator $\hat{T}_J(r, t_z)$ matrix elements for model space is the total of matrix elements of the one-body density (OBDM) $X_{J_f J_i}^J(t_z, j_i, j_f)$ times the elements of single particle matrix. It is determined by

$$\langle J_f || \hat{T}_{J:t_Z} || J_i \rangle = \sum_{j_i j_f} X_{J_f J_i}^J(t_z, j_i, j_f) \langle j_f || \hat{T}_{J:t_Z} || j_i \rangle \tag{3}$$

where j_i and j_f specify different single-particle states in the momentum space of shell model and t_z = 1/2 and -1/2 for a proton and a neutron respectively. On the other hand we use Skyrme force as a nucleon-nucleon effective interaction. This force consists of two parts, a two-body part and a zero-range three-body part [19], [20].

$$\hat{V}_{Skyrme} = \sum_{i<j} v_{ij}^{(2)} + \sum_{i<j<k} v_{ijk}^{(3)}, \tag{4}$$

where $v_{ij}^{(2)}$ is the two-body part and $v_{ijk}^{(3)}$ is the three-body part. The three-body part could be reduced to a two-body density dependent part. The Skyrme potential can be decomposed into its constituent terms

$$V_{Skyrme}(r_1;r_2) = t_0(1 + x_0 P_\sigma)\delta_{12}$$
$$+ \frac{t_1}{2}(1 + x_1 P_\sigma)(\delta_{12}k^2 + k'^2\delta_{12})$$
$$+ t_2\frac{t_1}{2}(1 + x_1 P_\sigma)k'\delta_{12}.k$$
$$+ \frac{t_3}{6}(1 + x_3 P_\sigma)p^\sigma(r)\delta_{12}$$
$$+ it_4(\sigma_1 + \sigma_2).k'\delta_{12}k \qquad (5)$$
$$+ \frac{t_e}{2}\{(3(\sigma_1.k')(\sigma_2.k') - (\sigma_1.\sigma_2)k'^2)\delta_{12}$$
$$+ \delta_{12}(3(\sigma_1.k)(\sigma_2.k) - (\sigma_1.\sigma_2)k^2)\}$$
$$+ t_o(3(\sigma_1.k')\delta_{12}(\sigma_2.k) - (\sigma_1.\sigma_2)k'.\delta_{12}k)$$

The term of t_3 coefficient is the three-body part and other terms are two-body part with $\delta_{12} = \delta\, r_1 - r_2$ and

$$k = \frac{1}{2i}(\bar{N}_1 - \bar{N}_2); k' = -\frac{1}{2i}(\bar{N}'_1 - \bar{N}'_2) \qquad (6)$$

The operators k and k' are the two nucleons relative wave vectors operates on the wave functions to the direction of right and left respectively and P^σ is the spin-exchange operator which is [21].

$$\sigma = \frac{1}{2}(1 + \sigma_1.\sigma_2) \qquad (7)$$

Putting two-body Skyrme interaction into Hartree-Fock equations gives a one body mean field potential. The neutron, proton, charge and mass densities can be determined by the relation [22].

$$\rho_k(r) = \sum_{n_\beta j_\beta l_\beta} w_\beta \frac{2j_\beta + 1}{4\pi} \left(\frac{R_\beta}{r}\right)^2; \qquad (8)$$

where $\frac{R_\beta}{r}$ denotes radial part, k represents neutron, proton, charge and mass, w_β is the probability of occupying the nucleon state β and j_β stand for total angular momentum of a nucleon in state β. The density distribution is a direct explore of the nucleus size, therefore the neutron, proton, charge and mass distributions r.m.s. radii can be calculated from the relation [23].

$$r_k = \langle r_k^2 \rangle^{1/2} = \left[\frac{\int_R^R r^4\rho_k(k)dr}{\int r^2\rho_k(k)dr}\right]^{1/2} \qquad (9)$$

The polarization of core (CP) charge density in CVTM model depends on the ground state charge density of the nucleus. The ground state charge density is expressed in terms of the two-body charge density for all occupied shells including

the core. The transition density of the core polarization of the Tassie shape is given by the collective modes of its nuclei [5].

$$\rho_{J;t_z}^{core}(i;f;r) = \frac{1}{2}C(1 + 2t_z)r^{J-1}\frac{d\rho_o(i;f;r)}{dr} \qquad (10)$$

where C is a constant of proportionality and ρ_0 is the charge density distribution for the ground state two- body.

Now the Coulomb form factor for this model becomes:

$$F_L^J = \left[\sqrt{\frac{4\pi}{2J_i + 1}}\frac{1}{Z}\int_0^\infty r^2 j_J(qr)\rho_{J;t_z}^{ms}(i;f;r)dr \right.$$
$$\left. + c\int_0^\infty j_J(qr)r^{J+1}\frac{d\rho_0(i;f;r)}{dr}dr\right] F_{cm}(q)F_{fs}(q) \qquad (11)$$

1.2 Results and discussion:

In the present study, we first found the one-body density matrices elements (OBDM) for the nucleons from Hartree-Fock equations putting Skyrme two-body interaction for SkXcsb and SLy4 parameterizations and using SM code NUSHELLX-@MSU [24]. Hence we calculated the Coulomb and transverse FFs for states of low-energy and positive parity of ^{17}O. Furthermore, the Tassie model has been utilized to account for CPE, which is calculating it from effective charges of nucleons [5]. The effective charges e_π = 1.5e for protons and e_v = 0.5e for neutrons have been adopted, it is tested very good for the sd shell [7]. The graphs were drawn using the Grapher program. Also, the finite size of nucleons has been considered in the computing the FFs. Besides the Skyrme interaction, the calculations for harmonic (HO) and Wood-Saxon (WS) single-particle potentials have been performed. The oscillator length constant b = 1.747 fm specified for HO potential. All calculations have been performed for ZBME model space, $1p_{1/2}$, $1d_{5/2}$, $2s_{1/2}$, $1d_{3/2}$ orbits, and rewile interaction which is a special interaction of NushellX@MSU program for this model space . Then we compared the results with experimental the data [8], [25]. We divided the results and discussion into the radius, the charge densities distribution and the FFs sections.

2. The Radius:

The results for proton, neutron, mass and charge r.m.s. radii for ^{17}O for four different potentials mentioned above are presented in Table 1 parallel to the experimental for charge radii [25]. As shown in the table, the calculated charge radii values for all potentials agree with the experimental, but the best is for HO potential. The values are 2.8366, 2.8967, 2.9274 and 2.8686 fm for HO, SkXcsb, SLy4 and WS interactions, respectively, while the measured value is 2.6932 fm.

Table 1. r.m.s. radii with unit fm for ^{17}O nucleus adopting some single-particle potentials.

Potential	Neutron	Proton	Mass	Charge	Charge exp. [25]
HO	2.7968	2.7198	2.7608	2.8366	2.6932
SkXcsb	2.8464	2.7810	2.8158	2.8967	
SLy4	2.8810	2.8132	2.8493	2.9274	
WS	2.8148	2.7518	2.7853	2.8686	

3. The Charge Densities Distribution:

The variation of charge density with distance from the nucleus center is shown in Figure 1. The results for Skyrme (SkXcsb and SLy4 parameterization) and HO interaction have constant region from center to 1.5 fm at 0.07 and 0.075 fm^{-3} respectively, then they drop until become zero at 5.3 fm. But the calculated values of WS have increased during center to 1.7 fm from 0.068 to 0.071 fm^{-3}, then have decreased to zero in the corresponding region r = 1.7 to 5.3 fm.

4. The Form Factors:

The calculations were performed only for low-energy positive parity states for the Coulomb and magnetic FFs.

4.1 Form Factors of Ground state, $J^{\pi} = 5{=}2^{+}$,

The ^{17}O ground state spin and parity of is $5{=}2^{+}$. From the rules of the summation of total angular momentum, $|J_i - J_f| \leq J \leq J_i + J_f$, and parity conservation, $(1)^J$ for Coulomb and $(1)^{J+1}$ for magnetic, the allowed multipole values of Coulomb (or longitudinal) and transverse magnetic FFs are C0, C2, C4, and M1, M3, M5 respectively. The scattering here is elastic since the nucleus remains in the ground state without excitement. This is because no energy transfers from the bombarding electron to the nucleus. In order to show the ESFFs dependence on potentials, the total ongitudinal and transverse magnetic FFs are found utilizing the complete ZBME model space for SLy4, SkXcsb parametrizations of Skyrme, HO, and WS potentials. Also, to know the quantitative contribution of the multipoles in producing total FF, we plot multipole projections parallelism to the totals. The multipoles are drown only for SkXcsb parametrization, which they are C2, C4, M1, M3, and M5 multipoles. Notice that C0 is not plotted here, this is because the measured Coulomb values exist for a total of only C2 and C4 contributions. The totals are given by eq.(1) The graphs are shown in Figure 2.

For the longitudinal FF, Figure 2(a), which is performed at ground state, 0.0 MeV, there is a good agreement qualitatively and quantitatively by the calculated results for all potentials to the experimentals along all measured momentum transfer, q, values, although a small overvalue will be shown. In addition, during all q values except around 1.9 fm^{-1} the C2 multipole has the major contribution to the formation of the total longitudinal FF, and around 1.9 fm^{-1} the contribution dominated by
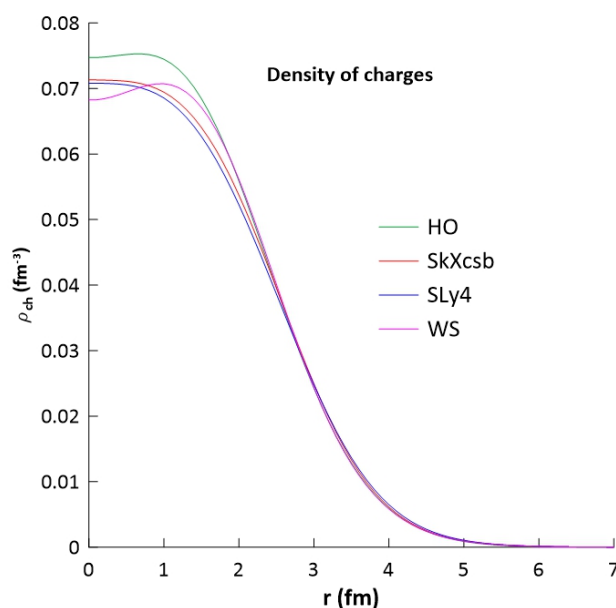

Figure 1. Charge spatial density distribution for ^{17}O nucleus using SkXcsb, SLy4 parameterization, HO and WS potentials.

C4 multipole. Also this agreement coming back to applying Tassie model for core polarization which generally has effect on the longitudinal form factors. For the transverse one, Figure 2(b), a very good consistency between all the potentials used with the experiment during all momentum transfer values will be shown, but the best one is SkXcsb parameterization. At low momentum transfer region, M1 multipole controls produce the total FF. At moderate region, each of M1, M3, and M5 contribution participates in making the total, and at high momentum transfer, just M5 dominates.

4.2 Form Factors of Positive parity excited states
4.2.1 Excited State $J^{\pi} = 1{=}2^{+}$:

For the J = $1{=}2$ state from the rules mentioned above, only the multipoles C2 for Coulomb and M3 for magnetic FFs are allowed. These are plotted in Figure 3. The scattering due to this state and others come after, is inelastic, since this leads to taking the nucleus from the ground to exited sates. Inelastic longitudinal C2 multipole FFs for the first $1{=}2^{+}$ state of ^{17}O at 0.870 MeV are demonstrated in Figure 3(a). In comparison with the measured taken data [8], one can see that the results for all potentials perfectly agree with the experimental data quantitatively and qualitatively at the low and intermediate region of q with a small underestimate. However, at high q region, they spread and were rather in agreement with the experimental one, and the HO was best of them. The inelastic magnetic M3 multipole is shown in Figure 3(b). Below 1.5 fm^1 momentum transfer, all potentials match with the experimental result except the HO one, which slightly shifts above and the best one is SkXcsb parameterization, from 1.5 up to 3
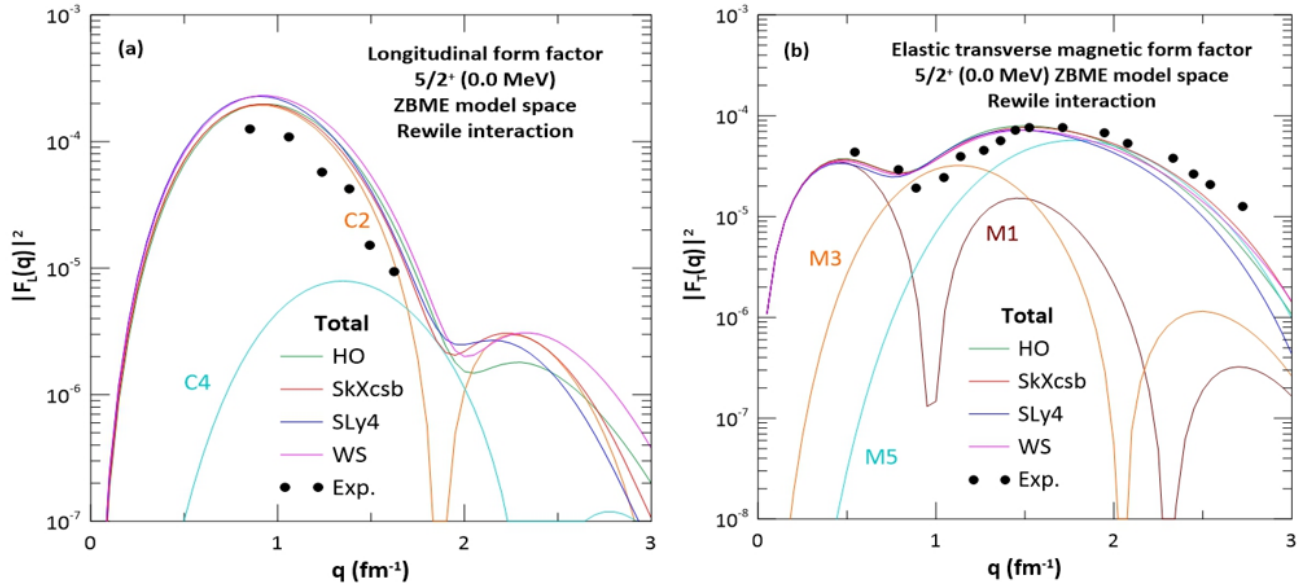
Figure 2. Theoretical elastic (a) longitudinal (b) transverse magnetic, FFs for the $5=2^+$, 0.0 MeV, ^{17}O nucleus state utilizing SkXcsb, SLy4 parameterization, HO and WS potentials. The experimental data taken from [8] also presented. The multipoles are displayed for SkXcsb parameterization.

fm^1 all potentials qualitatively are in good consistency with the measured values, but quantitatively they are a little below the measured values with the HO potential being their nearest to the experimental values. This discrepancy is due to the non-counting transverse electric contribution E2, which reproduces the total transverse FF together with M3 multipole.

4.2.2 Excited State $J^\pi = 3=2^+$:

In J = 3/2 state, we have C2 and C4 Coulomb multipoles. They belongs to 5.084 MeV state. The total FFs, CT = C2 + C4, are calculated for all potentials, but the different multipoles are only demonstrated for SkXcsb parametrization. The plots are illustrated in Figure 4 parallel to the experimental values. The predicted values rather have a different shape to the experimental values and overestimate them below 1.7 fm^{-1}, and underestimate above 2 fm^{-1}. But in the region 1.7 up to 2 fm^{-1} the predicted curves pass through the experiment ones. According to Alzubadi [7], this discrepancy is because the single-particle radial wave functions in the self-consistent mean field code are very good for the states of the holes but not for those of particles. Therefore excited states consists mainly by those particle states that may deliver uncertain FFs. Furthermore, in the results, there is a minimum, a bottom, near 1.9 fm^{-1} which is not exist in observed values. Along all q values region except around 1.9 fm^{-1} the C2 multipole has a dominant contribution in reproducing the total FFs, and around 1.9 fm^{-1} the total results made by C4 contribution.

4.2.3 Excited State $J^\pi = 7=2^+$:

In the $7=2^+$ excited state, the longitudinal C2 FF at 7.576 MeV is depicted in Figure 5. Obviously, the theoretical FF formed by the predicted ZBME model space has the same shape of the experimental curve with a small underestimate below 1.5 fm^{-1}. The experimental data do not exist above 2 fm^{-1} to comparison. The theoretical curves coincide together below this q value, but after that, they scatter. For all states, the FF curves relatively have a bell shape that is initially increase with q and then drop along it, this is according to eq. (2).

**4.2.4 Excited State $J^\pi = 9=2^+$:**

Finally, the Coulomb contribution C2 FFs for $9=2^+$ excited state at 8.470 MeV are plotted and shown in Figure 6. The calculated results quantitatively and qualitatively are a reasonable agreement to the experimental values, although there is a slightly overestimate below the momentum transfer 1.6 fm^{-1}.
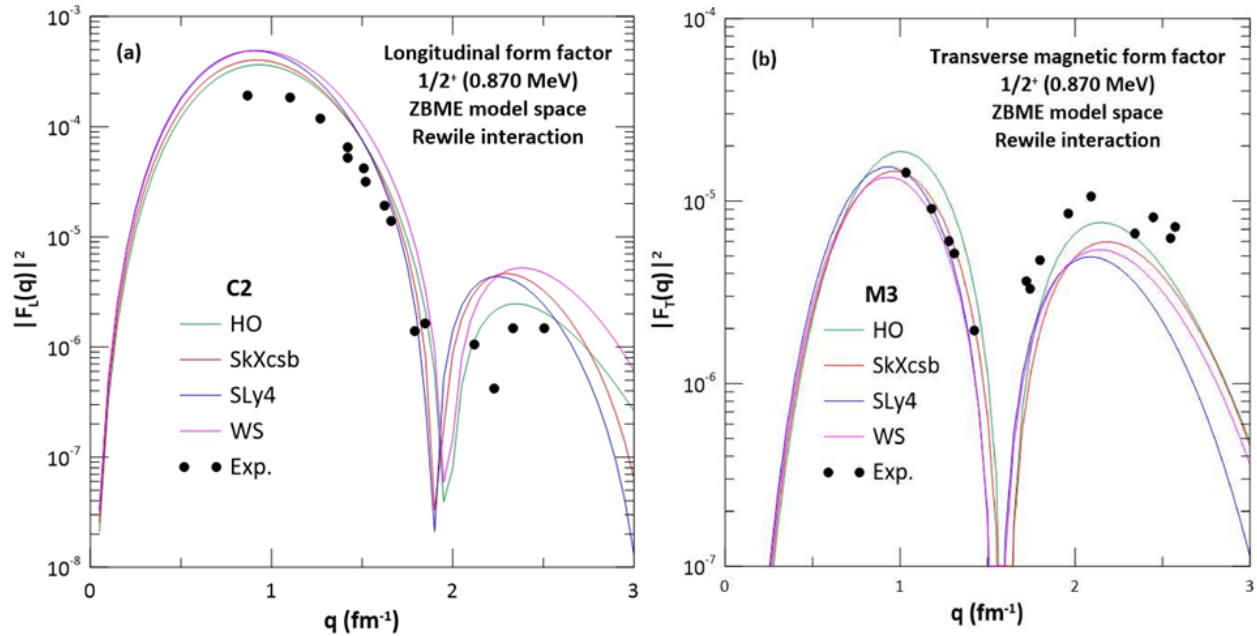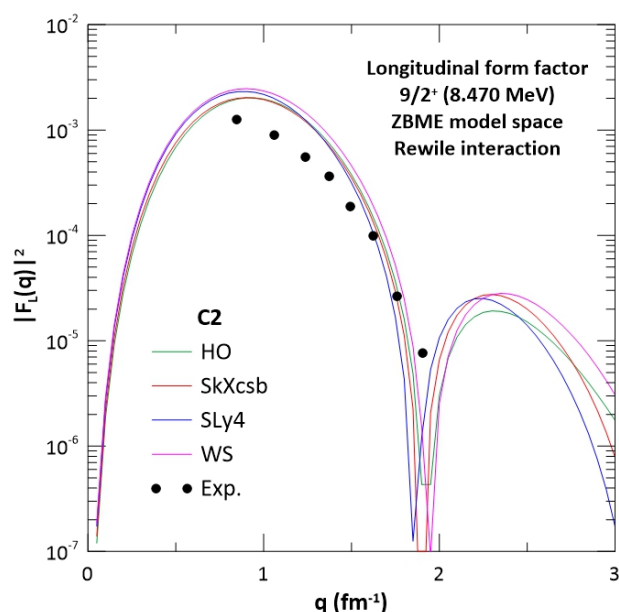
Figure 3. Theoretical FFs for the $1=2^+$, 0.870 MeV, ^{17}O nucleus state, (a) longitudinal C2 contribution (b) transverse magnetic M3 contribution, from SkXcsb, SLy4 parameterization, HO and WS potentials. To comparison the experimental data [8] are displayed.
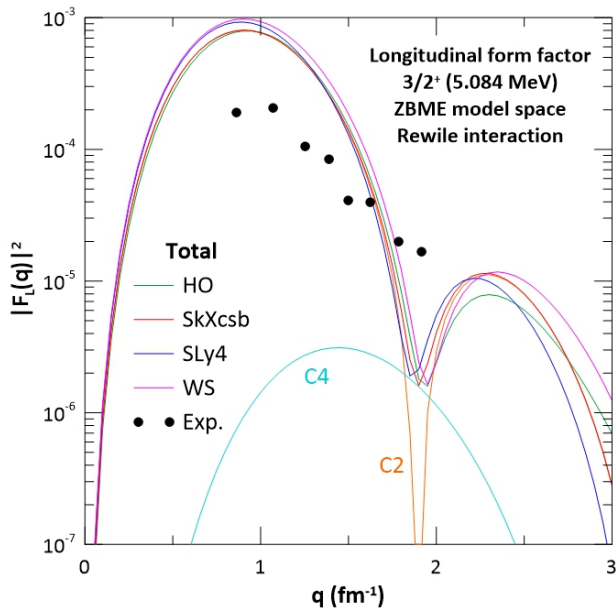
Figure 4. Theoretical elastic (a) longitudinal (b) transverse magnetic, FFs for the $5=2^+$, 0.0 MeV, ^{17}O nucleus state utilizing SkXcsb, SLy4 parameterization, HO and WS potentials. The experimental data taken from [8] also presented. The multipoles are displayed for SkXcsb parameterization.
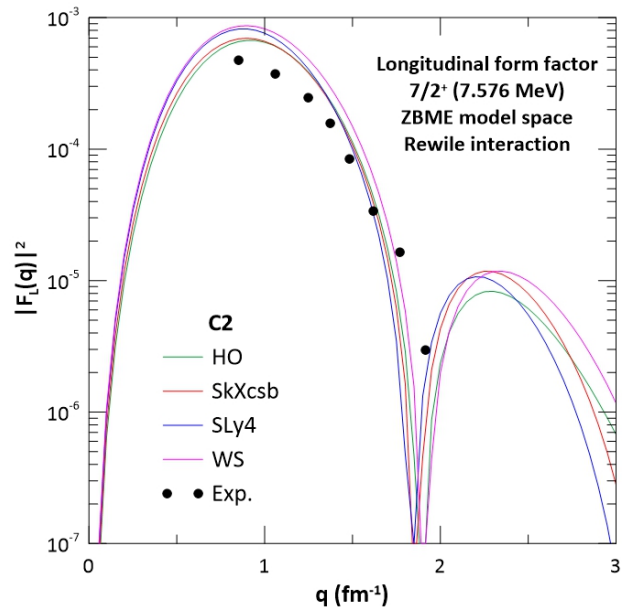
Figure 5. Theoretical longitudinal FFs for the $7=2^+$, 7.576 MeV, 17O nucleus state with C2 contribution addopting SkXcsb, SLy4 parameterization, HO and WS potentials. Nevertheless the observed data that [8] are presented.

Figure 6. Longitudinal C2 contribution theoretical FFs for the $9=2^+$, 8.470 MeV ^{17}O nucleus state by utilizing SkXcsb, SLy4 parameterization, HO and WS potentials. Parallel to the calculated values the measured data. [8] demonstrated.

5. Conclusion:

In the present work, we studied the structure of ^{17}O nucleus. From the results, we conclude that employing SHF calculations with SM are be able to describe the nuclear structure and properties, for instance, elastic and inelastic electron scattering form factors for low-lying positive parity states. Also Skyrme, HO, and WS potentials are very successful to represent effective nucleon-nucleon interactions, and give a reasonable form factor and charge radii to the experimental values, with the Skyrme one is the best. On the other hand, it is clear from the results that the HF method and equations can produce an appropriate mean field to the nucleons from Skyrme effective nucleon-nucleon interaction in the frame work of shell model for studying the nuclear structure. In general, The spatial behavior of the densities are be able to give by the three interactions. However, the constant characteristic near the nucleus center can be reproduced by the Skyrme

Data Availability Statement: All of the data supporting the findings of the presented study are available from correspond-ing author on request.

Declarations:
Conflict of interest: The authors declare that they have no conflict of interest.

Ethical approval: The manuscript has not been published or submitted to another journal, nor is it under review.

References

[1] Amritansshu Shukla and Suresh Kumar Patra. *Nuclear Structure Physics*. Tylor and Francis Group, 1st edition, 2021.

[2] W. A. Richter and B. A. Brown. Nuclear charge densities with the skyrme hartree-fock method. *Pysical Review C*, 67: 034317, 2003, doi:10.1103/PhysRevC.67.034317.

[3] R. A. Radhi, Ali A. Alzubadi, and Noori S. Manie. Electromagnetic multipoles of positive parity states in ^{27}Al by elastic and inelastic electron scattering. *Nuclear Physics A*, 1015: 122302, 2021, doi:10.1016/j.nuclphysa.2021.122302.

[4] A. K. Hamoudi, M. A. Hasan, and A. R. Ridha. Nucleon momentum distributions and elastic electron scattering form factors for some 1p-shell nuclei. *Pramana*, 78(5): 737–748, 2021, doi:10.1007/s12043-012-0269-6.

[5] S. J. Ahmad, K. S. Jassim, and F. A. Majeed. The effect of core polarization by means of tassie and bohr-mottelson models for some FP-shell nuclei. *Journal of Advanced Research in Dynamical and Control Systems*, 12(5): 200, 2021, doi:10.5373/JARDCS/V12I5/20201705.

[6] B. Waldman and G. B. Collins. Nuclear excitation of lead by X-rays. *Physical Review Journals Archive*, 57: 338–339, 1940, doi:10.1103/PhysRev.57.338.2.

[7] A. A. Alzubadi, R. A. Radhim, and N. S. Manie. Shell model and hartree-fock calculations of longitudinal and transverse electroexcitation of positive and negative parity states in ^{17}O. *Physical Review C*, 97: 024316, 2018, doi:10.1103/PhysRevC.97.024316.

[8] D. M. Manley, B. L. Berman, W. Bertozzi, T. N. Buti, J. M. Finn, F. W. Hersman, C. E. Hyde-Wright, M. V. Hynes, J. J. Kelly, M. A. Kovash, S. Kowalski, R. W. Lourie, B. Murdock, B. E. Norum, B. Pugh, and C. P. Sargent. High-resolution inelastic electron scattering from ^{17}O. *Physical Review C*, 36: 1700–1726, 1987, doi:10.1103/PhysRevC.36.1700.

[9] J. C. Kim, R. Yen, I. P. Auer, and H. S. Caplan. Low-lying octupole excitations in ^{17}O. *Physics Letters B*, 57(4): 341–344, 1975, doi:10.1016/0370-2693(75)90466-9.

[10] M. V. Hynes, H. Miska, B. Norum, W. Bertozzi, S. Kowalski, F. N. Rad, C. P. Sargent, T. Sasanuma, W. Turchinetz, and B. L. Berman. Electron scattering from the ground-state magnetization distribution of ^{17}O. *Physical Review Letters*, 42(22): 1444, 1979, doi:10.1103/PhysRevLett.42.1444.

[11] G. Bohannon, L. Zamick, and E. M. de Guerra. Structural considerations for elastic magnetic electron-nucleus scattering. *Nuclear Physics A*, 334(2): 278–296, 1980, doi:10.1016/0375-9474(80)90069-X.

[12] S. A. Coon and L. Jaqua. Wave function effects and the elastic magnetic form factor of ^{17}O. *Physical Review C*, 44(1): 203, 2022, doi:10.1103/PhysRevC.44.203.

[13] R.A. Radhi, N.T. Khalaf, and A.A. Najim. Elastic magnetic electron scattering from ^{17}O, ^{25}Mg and ^{27}Al. *Nuclear Physics A*, 75(11): e14675, 2021, doi:10.1016/S0375-9474(03)01009-1.

[14] J. L. Han, Q. Wang, Z. G. Xiao, H. S. Xu, Z. Y. Sun, Z. G. Hu, X. Y. Zhang, H. W. Wang, R. S. Mao, X. H. Yuan, and Z. G. Xu. Exotic behavior of elastic scattering differential cross-sections of weakly bound nucleus f-17 at small angles. *High energy physics and nuclear physics*, 30(11): 1058–1061, 2006.

[15] E. Strano, D. Torresi, M. Mazzocco, N. Keeley, A. Boiano, C. Boiano, P. Di Meo, A. Guglielmetti, M. La Commara, P. Molini, and C. Manea. ^{17}O+^{58}Ni scattering and reaction dynamics around the coulomb barrier. *Physical Review C*, 94(2): 024622, 2016, doi:10.1103/PhysRevC.94.024622.

[16] S. A. Abbas and K. H. Mahdi. The effects of core-polarization on the form factors of ^{17}O, ^{19}F and ^{48}Ca. *In IOP Conference Series: Materials Science and Engineering*, 871(1): 012092.

[17] MN. El-Hammamy, NA. El-Nohy, M. El-Azab Farid, S Diab, and Moamen M. El-Sayed. Systematic analysis of ^{17,19}F and ^{16,17}O elastic scattering on ^{208}Pb just below the coulomb barrier. *Chinese Journal of Physics*, 73: 136–146, 2021, doi:10.1016/j.cjph.2021.03.027.

[18] Shayma'a H. A., Ahmed A. A., and Ali H. Taqi. Effect of incompressibility and symmetry energy density on charge distribution and radii of closed-shell nuclei. *Kirkuk University Journal-Scientific Studies*, 17(3): 17–28, 2022, doi: 10.32894/KUJSS.2022.135889.1073.

[19] X. Pan, Y. T. Zou, H. M. Liu, B. He, X. H. Li, X. J. Wu, and Z. Zhang. Systematic study of two-proton radioactivity half-lives using the two-potential and skyrme-hartree-fock approaches. *Chinese Physics C*, 45(12): 124104, 2021, doi: 10.1097/CRD.000000000000330.

[20] Ali H. T. and Abdullah H. I. Collective excitations of 14n and 10b nuclei. *Kirkuk University Journal-Scientific Studies*, 11(1): 202–212, 2016, doi: 10.32894/KU-JSS.2016.124396.

[21] E. B. Suckling. *Nuclear structure and dynamics from the fully unrestricted Skyrme-Hartree-Fock model*. University of Surrey, United Kingdom, 2011.

[22] M. Vallières, H. Wu, (auth.), Prof. H. Langanke, Prof. A. Joachim Maruhn, and (eds.) Prof. S. E. Koonin. *Computational Nuclear Physics 1: Nuclear Structure*. Springer-Verlag Berlin Heidelberg, 1991.

[23] H. Aytekin, E. Tel, R. Baldik, and A. Aydin. An investigation for ground state features of some structural fusion materials. *Journal of Fusion Energy*, 30(1): 21–25, 2011, doi:10.1007/s10894-010-9326-7.

[24] BA Brown and WDM Rae. The shell-model code nushellx@ msu. *Nuclear Data Sheets*, 120: 115–118, 2014, doi: 10.1016/j.nds.2014.07.022.

[25] Krassimira Marinova and Istvan Angeli. Nuclear charge radii. *International Atomic Energy Agency*, 99: 69–95, 2013, doi: 10.1016/j.adt.2011.12.006.

Skyrme – Hartree Fock - ḥXñẞ éℂfₐ Ḳ ^{17}O èₐ Ĵ éJḳ ñ @ÉḲAÒJÉ HBẠ É¾, Ë@ÉÓₐ« éf X

hAJ¯ ŒₑkPéÔg ŒKŒ« * ,YÒₘ ÈñfP P @

.†@ª Ë@,éJḲAÒJÉ, Ë@,éJḲAÒJÉ, Ë@éª ÓAg ,Ðñ ª Ë@éJÊ¿ ,ZAK ^{Q} Ë@Œₑ„¯

aziz:fatah@univsul:edu:iq :Èðñ, @I kAḶ É@*

é" Cₙ'@

†Aℂ ú¯ éJÉₐ Ë@ð ÉḲAÒJÉ@éJḳ ñÓ HАKñJ, ÒÉÉ ^{17}O èₐ Ĵ éḲŒ @ ^{Q} «ð éḲŒ @éJ ð ^{Q} Ë B@ PAℂJfB@ É¾, ÉÓ « éf X I ẞ

¡fñJ @PYg HА, k Õç' A' @ *Skyrme – Hartree – Fock* HАKА, kð Œₐ„ Ë@ ḥXñẞ PA É@ú¯ $0.05 – 3$ fm^{-1} ÑkŒÉ@È №Ḳ@

$^©Ó$ ^{12}C èₐK áÓ hPAₙ'@(*ZBME*) ḥXñẞ ZA'¯ Ð YjJf@Œç' Y Ë .éJj, Ë@ éJ°Ë@ HАŒŒKñJJÉ@ð HАKñ ^{Q} Ë@áÓ É¾É ù ªJḲ ^{Q} Ë@

$^©Ó$,éJ JîÐ @ð úₐ•PB@ HАKñJ, @HBАg $^©$ JÒₘ *Sly*4 , *SkXscb* éÔ ª Ó $^©Ó$ ú× ^{Q} ^Óf HℂℂA K XAÒJ«@Œç' . (*rewile*) É«A K

é¯ñ $^®¯$ Ó Œₐ•AJ« HА, k úÍAJÉAḲ ð Yₑₙ'@¡fñJÓ YJÉñJÉ *Hartree – Fock* éḲŒℂ ú¯ *Wood – saxon* Yêkð ù $^®¯$ ₐ Ĵ É@Yₑₙ'@áÓ Ò'

éₘ• áÓ ‡ $^®¯$ j JÉÉ ,@g@úₐA fB@HАℂ $^®$ JfB@ ^{Q} KАK HА, ₙ (*Tassie*) úₐ.AK ḥXñẞ AJÓYjJf@AÒ».É¾, Ë@ÉÓ «ð ØXŒ Ë@Œₑ, ₙ'@

‡¯ₐK úî« Èñ'ₙ'@Œç' .AJ Œₘ' éfA $^®¯$ @Œₑₑ KАK AîÐKPA $^®$ ð AîÐ, ¯AJÓ I ẞ É¾, Ë@ÉÓ «ð , $^©$ JK ^{Q} Ë@¡fñJÓ PYg àA¯ ,éḲñ, j @Œₑ Ë@

.éfA $^®¯$ Ë@I 'AJJÉ@$^©$ Ó éḲŒℂJÉ@I 'AJJÉ@éḲPA $^®$ Ó ÈCg áÓ YJḳ

.É¾, Ë@ÉÓA« ;úₐ.AK ḥXñẞ ;¼ñ¯ŒKАë é $^®¯$ KŒƐ ;ú× ^{Q} ^Óf É«A K ;Œₐ„ Ë@ḥXñẞ ;àð ^{Q} Ë@ PAℂJf@:éƐₑYË@HАΟÊ¾Ë@

.YgñKB :ÉKñÒJÉ@

.Èðñ, @–Ëñ @áÓ AîÐÊƐ á°ẞ éÓY $^®¯$ @éf YÉ@I 'AJJÉ é «ₑYË@HАKАJJÉ@ $^©$ JÔg :HАKАJJÉ@^{Q} ¯ñK àAḳ

:H $^{P}0$ @¯

.Ì 'A' @ú¯ HPA' Ñî EYƐ • Ë éḲ@àñ $^®$ ËñŒ@Õ $^®$ K :Ì 'A' @HPA'

.éª ḳ @Œ @YJ¯ I , Ë AîË@AÒ» ,ØŒk@éÊj Œ Aê Y $^®$ K ð@é£ñℂj @Œₐ„ Œₑ K Œ :éJ¯ CgB@é $^®¯$ ₐ @